Multiple Model Adaptive Wave Filtering for Dynamic Positioning of Marine Vessels

Vahid Hassani, Asgeir J. Sørensen, António M. Pascoal and A. Pedro Aguiar

Abstract— **This paper addresses a filtering problem that arises in the design of dynamic positioning systems for ships and offshore rigs subjected to the influence of sea waves. Its key contribution is twofold: i) it introduces an improved model for filter design, and ii) and it exploits the structure of a multiple model adaptive wave filter that relies on measurements of the vessel's position and heading only. Namely, an improvement in the control plant model is proposed that better captures the physics of the problem at hand and a bank of Kalman filters is designed for a finite number of parameter values, each corresponding to a different peak frequency of the assumed wave spectrum model. Tools from multiple model adaptive estimation (MMAE) theory are exploited to blend the information provided by the different observers, yielding position and velocity estimates of the marine vessel. These estimates are then to be used in an appropriately designed feedback control law. Simulations illustrate the efficacy of the MMAE techniques proposed and the improvement in performance that is obtained when compared with other approaches.**

I. INTRODUCTION

Dynamic positioning (DP) systems came to existence in the 1960s for offshore drilling applications, due to the need to drill in deep waters and the realization that Jack-up barges and anchoring systems could not be used economically at such depths. Early dynamic positioning systems were implemented using PID controllers. In order to restrain thruster trembling caused by the wave-induced motion components, notch filters in cascade with low pass filters were used with the controllers. However, notch filters restrict the performance of closed-loop systems because they introduce phase lag around the crossover frequency, which in turn tends to decrease phase margin. An improvement in performance was achieved by exploiting more advanced control techniques based on optimal control and Kalman filter theory, see [1]. These techniques were later modified and extended in [2], [3], [4], [5], [6], [7], [8], [9], [10], [11] and [12]. For a survey of dynamic positioning control systems, see [13] and the references therein. One of the most fruitful concepts introduced in the course of the body of work referred above was that of wave filtering, together with the strategy of modeling the total vessel motion as the superposition of low-frequency (LF) vessel motion and wave-frequency (WF) motions. It was further recognized that in order to reduce the mechanical wear and tear of the propulsion system components, in small to high see states, the estimates entering the DP control feedback loop should be filtered by using a so-called wave filtering technique so as to prevent excessive control activity in response to WF components. In practice, position and heading measurements are corrupted not only with sensor noise but also with colored noise caused by wind, waves, and ocean currents; thus the need for an observer to achieve wave filtering and "separate" the LF and WF position and heading estimates (see [14] for details). In extreme seas or swell with very long wave periods, wave filtering is turned off as described in [13] and [15].

In [8], WF filtering was done by exploiting the use of Kalman filter theory under the assumption that the kinematic equations of the ship's motion can be linearized about a set of predefined constant yaw angles (36 operating points in steps of 10 degrees, covering the whole heading envelope); this is necessary when applying linear Kalman filter theory and gain scheduling techniques. However, global exponential stability (GES) of the complete system cannot be guaranteed. In [16], a nonlinear observer with wave filtering capabilities and bias estimation was designed using passivity. An extension of this observer with adaptive wave filtering was described in [17]. Gain-scheduled wave filtering was introduced in [12].

Except for the work in [17], [12], [15], and [18], the design techniques mentioned so far assume that sea state (and the WF model parameters) do not change during operation and that the WF model parameters are known a priori. In practice, the sea state may undergo large variations and therefore the observer in charge of reconstructing the LF motion should adapt to the sea state itself. The nonlinear passive observer technique introduced in [17] for recursive adaptive filtering is a very important contribution towards meeting the above goal. However, the task of filter tuning may meet with difficulties. In [12] and [15] the observer gains were parameterized by the wave peak frequencies and spectral analysis techniques were used to estimate the wave spectrum in surge, sway, and yaw from position and heading measurements. This approach is sensitive to measurement noise and may have latency problems because it requires that the samples acquired be buffered to estimate the Power Density Spectrum of the measurement time series.

In this paper, inspired by previous pioneering work on DP, a modified model for wave filtering is proposed; in addition, based on the adopted model we propose the use of a multiple model adaptive wave filter that relies on measurements of the vessel's position and heading only. To this effect, a bank of

This work was supported in part by projects MORPH (EU FP7 under grant agreement No. 288704) and CONAV/FCT-PT (PTDC/EEA-CRO/113820/2009) and the FCT [PEst-OE/EEI/LA0009/2011] and was carried out in cooperation with the Centre for Ships and Ocean Structures (CeSOS); the Norwegian research council is acknowledged as the main sponsor of CeSOS. The first author benefited from grant SFRH/BD/45775/2008 of the Foundation for Science and Technology (FCT), Portugal.

Vahid Hassani, António M. Pascoal and A. Pedro Aguiar are with Institute for Systems and Robotics (ISR), Instituto Superior Técnico (IST), Lisbon, Portugal. Tel: (+351) 21 841 8054, Fax: (+351) 21 841 8291 {vahid,antonio,pedro}@isr.ist.utl.pt

Asgeir J. Sørensen is with Centre for Ships and Ocean Structures (CeSOS) and Dept. of Marine Technology, Norwegian Univ. of Science and Technology, Trondheim, Norway, asgeir.sorensen@ntnu.no.

Kalman filters is designed for a finite number of parameter values, each corresponding to a different peak frequency of the assumed wave spectrum model. The main emphasis of the paper is on the new adopted model and the use of a multiple model scheme for adaptive wave filtering; however, for the sake of completeness, in the numerical simulations a multivariable PID is used to control the position of the vessel.

The structure of the local observers builds upon steady state Kalman filters; see [19]. Tools from multiples model adaptive estimation (MMAE) theory are exploited to blend the information provided by the different observers, yielding position and velocity estimates of the vessel. For the necessary background information and the mathematical framework used in the analysis and design of MMAE filters the reader is referred to [20], [21], [22], [23], [18], and the references therein. In the set-up adopted, the observers run in parallel and at each instant of time their residuals are used to compute, for each observer, the probability that the peak frequency of the assumed wave spectrum model is the true peak frequency of the wave disturbing the vessel motion. The state estimate is a probabilistically weighted combination of each observer estimate.

The structure of the paper is as follows. Section II is a brief introduction to important issues that arise in DP. Moreover, a modified representative vessel model is proposed. Section III summarizes the main ideas behind MMAE; it also reviews the basic structure of local observers. An example is described in Section IV that illustrates the strategy proposed, via computer simulations. Conclusions and suggestions for future research are summarized in Section V.

II. DYNAMIC POSITIONING: FILTERING AND SHIP MODELING

In DP systems, the key objective is to maintain the vessel's heading and position within desired limits. Central to their implementation is the availability of good heading and position estimates, provided by properly designed filters. In general, measurements of the vessel velocities are not available and measurements of position and heading are corrupted with different noises. Consequently, estimates of the velocities must be computed from corrupted measurements of position and heading through a state observer. Furthermore, only the slowly-varying disturbances should be counterbalanced by the propulsion system, whereas the oscillatory motion induced by the waves (1st-order wave induced loads) should not enter the feedback control loop. To this effect, the DP control systems should be designed so as to react to the low frequency forces on the vessel only. As mentioned, wave filtering techniques are exploited to separate the position and heading measurements into low-frequency (LF) and wave-frequency (WF) position and heading estimates. Fig. 1 illustrates this concept graphically. It was this interesting circle of ideas that motivated the work reported in the present paper on multiple model adaptive wave filtering.

In what follows, the vessel model, that is by now standard, is presented. See [16], [12], [24]. The model admits the

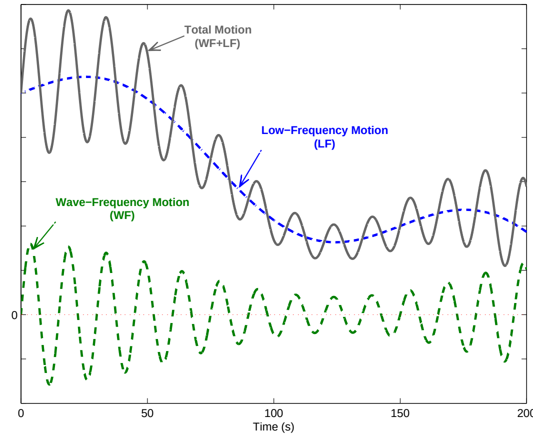

Fig. 1. The total motion of a ship is modeled as a LF response with the WF motion added as an output disturbance (adopted from [16], [24]).

realization

$$\dot{\xi}_\omega = A_\omega(\omega_0)\xi_\omega + E_\omega w_\omega \tag{1}$$
$$\eta_\omega = C_\omega \xi_\omega \tag{2}$$
$$\dot{b} = -T^{-1}b + E_b w_b \tag{3}$$
$$\dot{\eta}_L = R(\psi_L)\nu \tag{4}$$
$$M\dot{\nu} + D\nu = \tau + R^T(\psi_{tot})b \tag{5}$$
$$\eta_{tot} = \eta_L + \eta_\omega \tag{6}$$
$$\eta_y = \eta_{tot} + v \tag{7}$$

where (1) and (2) capture the 1st-order wave induced motion in surge, sway, and yaw; equation (3) represents the 1st-order Markov process approximating the unmodelled dynamics and the slowly varying bias forces (in surge and sway) and torques (in yaw) due to waves (2nd order wave induced loads), wind, and currents, where the latter are given in earth fixed coordinates but expressed in body-axis. The vector $\eta_\omega \in \mathbb{R}^3$ is the vessel's WF motion due to 1st-order wave-induced disturbances consists of, WF position, (x_W, y_W) and WF heading ψ_W of the vessel; $w_\omega \in \mathbb{R}^3$ and $w_b \in \mathbb{R}^3$ are zero mean Gaussian white noise vectors, and

$$A_\omega = \begin{bmatrix} 0_{3\times3} & I_{3\times3} \\ -\Omega_{3\times3} & -\Lambda_{3\times3} \end{bmatrix}, \qquad E_\omega = \begin{bmatrix} 0_{3\times1} \\ I_{3\times1} \end{bmatrix},$$
$$C_\omega = \begin{bmatrix} 0_{3\times3} & I_{3\times3} \end{bmatrix},$$

with

$$\Omega = \mathrm{diag}\{\omega_{01}^2, \omega_{02}^2, \omega_{03}^2\},$$
$$\Lambda = \mathrm{diag}\{2\zeta_1\omega_{01}, 2\zeta_2\omega_{02}, 2\zeta_3\omega_{03}\},$$

where ω_{0i} and ζ_i are the Dominant Wave Frequency (DWF) and relative damping ratio, respectively. Matrix $T = \mathrm{diag}(T_x, T_y, T_\psi)$ is a diagonal matrix of positive bias time constants and $E_b \in \mathbb{R}^{3\times3}$ is a diagonal scaling matrix. The vector $\eta_L \in \mathbb{R}^3$ consists of low frequency (LF), earth-fixed position (x_L, y_L) and LF heading ψ_L of the vessel relative to an earth-fixed frame, $\nu \in \mathbb{R}^3$ represents the velocities decomposed in a vessel-fixed reference, and $R(\psi_L)$ is the standard orthogonal yaw angle rotation matrix (see [14] for details). Equation (5) describes the vessels's LF motion at low speed (see [14]), where $M \in \mathbb{R}^{3\times3}$ is the generalized system inertia matrix including zero frequency added mass components, $D \in \mathbb{R}^{3\times3}$ is the linear damping matrix, and $\tau \in \mathbb{R}^3$ is a control vector of generalized forces generated by the propulsion system, that is, the main propellers aft of the ship and thrusters which can produce surge and sway forces as well as a yaw moment. The vector $\eta_{tot} \in \mathbb{R}^3$ is the vessel's total motion, consists of total position (x_{tot}, y_{tot}) and total heading ψ_{tot} of the vessel. Finally (7), represents the position and heading measurement equation, $v \in \mathbb{R}^3$ is zero-mean Gaussian white measurement noise.

Clearly, in the model described in (1)-(7) the evolution of the WF components of the motion, (1), (2) and (7), are modeled as a 2nd-order linear time invariant (LTI) system, driven by Gaussian white noise, in earth-fixed frame.

It is commonly accepted in station keeping operations, assuming small motions about the coordinates η_d (x_d, y_d, and ψ_d), that the coupled equations of WF motions can be formulated in the hydrodynamic frame with[1]

$$M(w)\ddot{\eta}_{R\omega} + D_p(w)\dot{\eta}_{R\omega} = \tau_{\text{wave1}} \tag{8}$$

$$\dot{\eta}_\omega = R(\psi)\dot{\eta}_{R\omega} \tag{9}$$

where $\eta_{R\omega} \in \mathbb{R}^3$ is the WF motion vector in the hydrodynamic frame, $\eta_\omega \in \mathbb{R}^3$ is the WF motion vector in the Earth-fixed frame and $\tau_{\text{wave1}} \in \mathbb{R}^3$ is the first order wave excitation vector, which is dependent on the vessel heading relative to the incident wave direction. In the above, $M(w) \in \mathbb{R}^{3\times3}$ is the system inertia matrix containing frequency dependent added mass coefficients in addition to the vessel's mass and moment of inertia and $D_p(w) \in \mathbb{R}^{3\times3}$ is the wave radiation (potential) damping matrix. Here, it is assumed that the mooring lines, if any, will not affect the WF motion [25].

The above indicate that the WF motion should be computed in the hydrodynamic frame. We now recall that the problem of modeling the hydrodynamic forces applied to a vessel in regular waves is solved as two sub-problems: "wave reaction" (or wave radiation) and "wave excitation"; the forces calculated in each of these sub-problems can be added together to give the total hydrodynamic forces [26]. Potential theory is assumed, neglecting viscous effects. The following effects are important:

Wave Reaction: Forces and moments on the vessel when the vessel is forced to oscillate with the wave excitation frequency. The hydrodynamic loads are identified as added mass and wave radiation damping terms.

Wave Excitation: Forces and moments on the vessel when the vessel is restrained from oscillating and there are incident waves. This gives the wave excitation loads which are composed of so-called Froude-Kriloff (forces and moments due to the undisturbed pressure field as if the vessel were not present) and diffraction forces and moments (forces and moments because the presence of the vessel changes the pressure field).

Results from model tests and computer programs for vessel response analysis often come in the form of transfer functions or tables of coefficients. This can be applied to linear wave-induced motions, 2nd-order wave drift and slowly varying motions. To a large extent, linear theory is sufficient for describing wave-induced motions and loads on vessels. This is especially true for small to moderate sea states.

To this effect, a frequency spectrum $S(\omega)$ is selected to describe the energy distribution of the wind generated sea waves and swell over different frequencies, with the integral over all frequencies representing the total energy of the sea state. Common frequency spectra are the Pierson-Moskowitz (PM) spectrum, the ITTC/ISSC spectrum, the JONSWAP spectrum, and the more recent doubly peaked spectrum by Torsethaugen (for details see [14], [24] and references therein). Linear approximations to the wave spectra are studied in the literature; in particular, 2nd-order wave transfer function approximations have attracted considerable attention, see [2], [3], [4], [5], [6], [7], [8], [9], [10], [11], [12], and [15].

In this paper we also consider a 2nd-order wave transfer function approximation and we propose a modified model for the WF components of motion as follows:

$$\dot{\xi}_\omega = A_\omega(\omega_0)\xi_\omega + E_\omega w_\omega \tag{10}$$

$$\eta_\omega = R(\psi_L)C_\omega\xi_\omega \tag{11}$$

$$\dot{b} = -T^{-1}b + E_b w_b \tag{12}$$

$$\dot{\eta}_L = R(\psi_L)\nu \tag{13}$$

$$M\dot{\nu} + D\nu = \tau + R^T(\psi_{tot})b \tag{14}$$

$$\eta_{tot} = \eta_L + \eta_\omega \tag{15}$$

$$\eta_y = \eta_{tot} + v \tag{16}$$

where all the variables are as defined in (1)-(7). At this point we would like to highlight the difference between (2) and (11). As mentioned before, the evolution of the WF components of the motion in (1), (2) and (7), are modeled as a 2nd-order linear time invariant (LTI) system, derived with Gaussian white noise, in earth-fixed frame, while (8) suggests to model the WF motions in a body frame. From a physical point of view, it is obvious that the WF motions depend on the angle between the heading of the vessel and the direction of the wave. Assuming stationary waves,[2] one can assume that a linear approximation can be used to described wave-induced motions in the body frame. This justifies the modification applied in (11). Modeling the WF motions in earth-fixed frame means that every time a new command for a desired heading is issued, the WF motion dynamic should be updated. By modeling the WF motion dynamic in body frame such a problem will not occur.

A. Designing Observers

When designing an observer for wave filtering, the following assumptions are made (these assumptions are widely used in the literature, see [10], [17], [11], [27], [12]):

Assumption 1 Position and heading sensor noise are neglected, that is $v = 0$, since the measurement error induced by induced by measurement noise is negligible compared to

[1]In 6DOF dynamics, the equation (8) changes to $M(w)\eta\ddot{R}_\omega + D_p(w)\dot{\eta}_{R\omega} + G\eta_{R\omega} = \tau_{\text{wave1}}$, where $G \in \mathbb{R}^{6\times6}$ is the linearized restoring coefficient matrix due to the gravity and buoyancy affecting heave, roll and pitch only (see [24] for details). Throughout this paper a 3DOF dynamics is used for the purpose of design while a 6DOF dynamics is used in the simulation.

[2]In long-crested irregular sea, the sea elevation can be assumed statistically stable. See [24] for details and differences in Long- and Short-Crested Seas.

the wave-induced motion.

Assumption 2 The amplitude of the wave-induced yaw motion ψ_ω is assumed to be small, that is, less than 2-3 degrees during normal operation of the vessel and less than 5 degrees in extreme weather conditions. Hence, $R(\psi_L) \approx R(\psi_L + \psi_W)$. From Assumption 1 it follows that $R(\psi_L) \approx R(\psi_y)$, where $\psi_y \cong \psi_L + \psi_W$ denotes the measured heading.

Assumption 3 Low speed assumption, where the time-derivative of the total heading $\dot{\psi}_{tot}$ is small, bounded, and close to zero.

We will also exploit the model property that the bias time constant in the x and y directions are equal, i.e. $T_x = T_y$.

Let us define a new coordinates of *vessel parallel coordinates* as introduced in [14], [24] and [28]. Vessel parallel coordinates are defined in a reference frame fixed to the vessel, with axes parallel to the earth-fixed frame. Vector $\eta_L^p \in \mathbb{R}^3$ consists of the LF position (x_L^p, y_L^p) and LF heading ψ_L^p of the vessel expressed in body coordinates, defined as

$$\eta_L^p = R^T(\psi_{tot})\eta_L. \tag{17}$$

Computing its derivative with respect to time yields

$$\begin{aligned} \dot{\eta}_L^p &= \dot{R}^T(\psi_{tot})\eta_L + R^T(\psi_{tot})\dot{\eta}_L \\ &= \dot{R}^T(\psi_{tot})R(\psi_{tot})\eta_L^p + R^T(\psi_{tot})R(\psi_L)\nu. \end{aligned} \tag{18}$$

Using a Taylor series to expand $R^T(\psi_{tot})$ about ψ_L and neglecting the higher order terms, it follows that

$$R^T(\psi_{tot})R(\psi_L) \cong I + \psi_W S, \tag{19}$$

where

$$S = \begin{bmatrix} 0 & 1 & 0 \\ -1 & 0 & 0 \\ 0 & 0 & 0 \end{bmatrix}.$$

Using simple algebra we obtain

$$\dot{R}^T(\psi_{tot})R(\psi_{tot}) = \dot{\psi}_{tot} S. \tag{20}$$

From (18), (19) and (20) we conclude that

$$\dot{\eta}_L^p \approx \dot{\psi}_{tot} S \eta_L^p + \nu + \psi_W S \nu. \tag{21}$$

We now study the time evolution of the slowly varying bias forces, b, expressed in the in the vessel parallel coordinates, b_p, as follows:

$$b^p = R^T(\psi_{tot})b. \tag{22}$$

Clearly,

$$b = R(\psi_{tot})b^p, \tag{23}$$

and differentiating from both sides yields

$$\dot{b} = \dot{R}(\psi_{tot})b^p + R(\psi_{tot})\dot{b}^p. \tag{24}$$

Recalling (12), (23) and (24) we now have

$$\dot{R}(\psi_{tot})b^p + R(\psi_{tot})\dot{b}^p = -T^{-1}R(\psi_{tot})b^p + E_b w_b. \tag{25}$$

Reordering (25) and multiplying both sides by $R^T(\psi_{tot})$ gives

$$\begin{aligned} \dot{b}^p = &-R^T(\psi_{tot})T^{-1}R(\psi_{tot})b^p - R^T(\psi_{tot})\dot{R}(\psi_{tot})b^p \\ &+ R^T(\psi_{tot})E_b w_b. \end{aligned} \tag{26}$$

Using the assumption that $T_x = T_y$, it can be checked that $R^T(\psi_{tot})T = TR^T(\psi_{tot})$; simple algebra also shows that $R^T(\psi_{tot})\dot{R}(\psi_{tot}) = -\dot{\psi}_{tot}S$.

Equation (26) can be expressed as

$$\dot{b}^p = -T^{-1}b^p + \dot{\psi}_{tot} S b^p + R^T(\psi_{tot})E_b w_b. \tag{27}$$

Summarizing the equations above yields

$$\dot{\xi}_\omega = A_\omega(\omega_0)\xi_\omega + E_\omega w_\omega \tag{28}$$
$$\eta_\omega = R(\psi_L)C_\omega \xi_\omega \tag{29}$$
$$\dot{b}^p = -T^{-1}b^p + \dot{\psi}_{tot} S b^p + R^T(\psi_{tot})E_b w_b \tag{30}$$
$$\dot{\eta}_L^p = \dot{\psi}_{tot} S \eta_L^p + \nu + \psi_W S \nu \tag{31}$$
$$M\dot{\nu} + D\nu = \tau + b^p \tag{32}$$

Moreover, using assumptions 1, 2 and 3 a linear model is obtained that is given by

$$\dot{\xi}_\omega = A_\omega(\omega_0)\xi_\omega + E_\omega w_\omega \tag{33}$$
$$\eta_\omega^b = C_\omega \xi_\omega \tag{34}$$
$$\dot{b}^p = -T^{-1}b^p + w_b^f \tag{35}$$
$$\dot{\eta}_L^p = \nu \tag{36}$$
$$M\dot{\nu} + D\nu = \tau + b^p \tag{37}$$
$$\eta_y^f = \eta_L^p + \eta_\omega^b \tag{38}$$

where η_ω^b are WF components of motion on body-coordinate axis, and w_b^f and η_y^f are a new modified disturbance and a modified measurement defined by $w_b^f = R^T(\psi_y)E_b w_b$ and $\eta_y^f = R^T(\psi_y)\eta_y$, respectively.[3]

III. The Continuous-Time Multiple-Model Adaptive Estimator

One of the earliest uses of multiple-models was motivated by the need to accurately estimate the state of a stochastic dynamic system subjected to significant parameter uncertainty. In many applications, the estimation accuracy provided by standard KFs was not adequate. This led to the consideration of Multiple Model Adaptive Estimation (MMAE) techniques. For some early references on Multiple-Model Adaptive Estimator see [29], [19], [30]. Fig. 2 shows the architecture of a MMAE system. It is assumed that a linear time-invariant plant G is driven by white noise and a known deterministic input signal and that it generates measurements that are corrupted by white measurement noise. If there is no parameter uncertainty in the plant, then the Kalman filter (KF) is the optimal state-estimation algorithm in a well-defined sense; see, for example, [19]. Moreover, under the usual linear-gaussian assumptions, the KF state-estimate is the true conditional mean of the state, given the past controls and observations. If the plant has an uncertain real-parameter vector, say ω_0, one can imagine that it is "close" to one of the elements of a finite discrete representative parameter set, $\Omega := \{\omega_0^1, \omega_0^2, \ldots, \omega_0^N\}$. One can then design a bank of standard KFs, where each KF uses one of the discrete parameters ω_0^i in its implementation, $i \in \{1, \ldots, N\}$. It turns

[3]When designing the observers for wave filtering in dynamic positioning, since the controller regulates the heading of the vessel, the designer can assign a new intensity to w_b^f; however, assigning the intensity of the noise in practice requires considerable expertise.

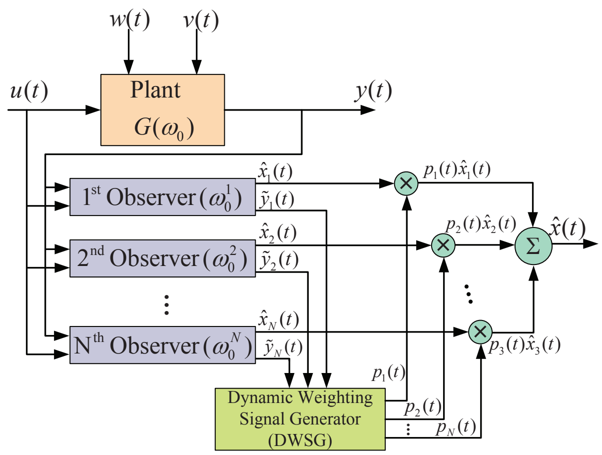

Fig. 2. The MMAE architecture.

out that, if indeed the true plant parameter is one of the discrete values, then the conditional probability density of the state is the sum of Gaussian densities. In this case, the multiple model adaptive estimator of Fig. 2 will generate the true conditional mean of the state, and one can compute the true conditional covariance matrix; see, for example, [19]. The structure of MMAE, in Fig. 2, consists of: i) the dynamic weighting signal generator (DWSG) and ii) a bank of N KFs, where each local estimator is designed based on one of the representative parameters. The state estimate is generated by a probabilistically weighted sum of the local state-estimates produced by the bank of KFs.

Multiple Model Adaptive Estimation for continuous time LTI systems was introduced in [31]. However, no proof of convergence of the state estimate or dynamic weights was given. Later on, in [32] and [33], a new approach to compute dynamic weights in a stochastic setup was presented. Again, no proof of convergence of the state estimate or the dynamic weights was offered. In [34], using the dynamic weights introduced previously in [32] and [33], it was shown for the first time that the estimation error is bounded; however, there was no proof of convergence of the dynamic weights. To tackle this problem, in [20] a different method was proposed to generate dynamic weights. Interestingly enough, with the reformulated expression for dynamic weights, convergence of the latter was proven under a certain distinguishability condition. It was further shown that the estimation error is bounded and converges to zero when the true plant parameter is one of the discrete values. The distinguishability condition was later relaxed in [23]. The reader will find in [23] a thorough discussion of convergence analysis when the actual plant parameter is not one of the discrete values adopted during the design phase.

In what follows, we assume the plant model G is subjected to parameter uncertainty $\omega_0 \in \mathbb{R}^l$, that is, $G = G(\omega_0)$. We consider multiple-input-multiple-output (MIMO) linear plant models of the form

$$\dot{x}(t) = A(\omega_0)x(t) + Bu(t) + Lw(t), \tag{39a}$$
$$y(t) = Cx(t) + v(t), \tag{39b}$$

where $x(t) \in \mathbb{R}^n$ denotes the state of the system, $u(t) \in \mathbb{R}^m$ its control input, $y(t) \in \mathbb{R}^q$ its measured noisy output, $w(t) \in \mathbb{R}^r$ an input plant disturbance that cannot be measured, and $v(t) \in \mathbb{R}^q$ is the measurement noise. Vectors $w(t)$ and $v(t)$ are zero-mean white Gaussian signals, mutually independent with intensities $E\{w(t)w^T(\tau)\} = Q\delta(t-\tau)$ and $E\{v(t)v^T(\tau)\} = R\delta(t-\tau)$. The initial condition $x(0)$ of (39) is Gaussian random vector with mean and covariance given by $E\{x(0)\} = 0$ and $E\{x(0)x^T(0)\} = \Sigma(0)$. Matrix $A(\omega_0)$ contains *unknown constant parameters* indexed by ω_0. Consider a finite set of candidate parameter values $\Omega = \{\omega_0^1, \omega_0^2, \ldots, \omega_0^N\}$ indexed by $i \in \{1, \ldots, N\}$. We propose the following MMAE. The state estimate is given by

$$\hat{x}(t) := \sum_{i=1}^{N} p_i(t)\hat{x}_i(t), \tag{40}$$

where $\hat{x}(t)$ is the estimate of the state $x(t)$ (at time t) and $p_i(t)$ is the conditional probability that $\omega_0 = \omega_o^i$, given the measurements record. In (40), each $\hat{x}_i(t)$; $i = 1, \ldots, N$ corresponds to a "local" state estimate generated by the i^{th} steady state Kalman filter ([19]),

$$\begin{aligned} 0 = {} & A(\omega_0^i)\Sigma_{\omega_0^i} + \Sigma_{\omega_0^i}A^T(\omega_0^i) + LQL^T \\ & - \Sigma_{\omega_0^i}C^T R^{-1} C \Sigma_{\omega_0^i}, \end{aligned} \tag{41a}$$
$$\dot{\hat{x}}_i(t) = A(\omega_0^i)\hat{x}_i(t) + Bu(t) + H_{\omega_0^i}\big(y(t) - C\hat{x}_i(t)\big), \tag{41b}$$
$$\hat{y}_i(t) = C\hat{x}_i(t), \tag{41c}$$

where $H_{\omega_0^i} = \Sigma_{\omega_0^i}C^T R^{-1}$ is the Kalman filter gain and $[A(\omega_0^i), L]$ and $[A(\omega_0^i), C]$ are assumed to be stabilizable and detectable, respectively for $i = 1, \ldots, N$.

In the sequel we introduce dynamic weights that weigh the local estimations (40). As mentioned before, the (stochastic) continuous-time MMAE (CT-MMAE) was introduced in [31], [32], [33]. A priori probabilities for each estimator were derived, but no convergence results were given either for the dynamic weights or the estimation error. In [20], the continuous counterpart of the weight generator that was introduced in discrete-time MMAE by [30], and [19] was used in the CT-MMAE structure for the first time. The new resulting structure shed light into the process of proving not only convergence of dynamic weights in the CT-MMAE but also boundedness of the estimation error. In this case, the dynamic weights are generated by a continuous time differential equation, the structure of which can be found in [20], [23]. This structure will be used in the sequel.

In the proposed MMAE, the dynamic weights $p_i(t) \in \mathbb{R}$, $i = 1, \ldots, N$ satisfy

$$\dot{p}_i(t) = -\lambda\Big(1 - \frac{\beta_i(t)e^{-m_i(t)}}{\sum_{j=1}^{N} p_j(t)\beta_j(t)e^{-m_j(t)}}\Big)p_i(t), \tag{42}$$

where λ is a positive constant, $\beta_i(t)$ is a signal assumed to satisfy the condition $c_1 \leq \beta_i(t) \leq c_2$ for some positive constants c_1, c_2, and $m_i(\cdot)$ is a continuous function called an *error measuring function* that maps the measurable signals of the plant and the states of the i^{th} local estimator to a nonnegative real value. An example of an error measuring function and a $\beta_i(t)$ function, which used throughout this paper, are $m_i(t) := \frac{1}{2}\|y(t) - \hat{y}_i(t)\|^2_{S_i^{-1}}$ and $\beta_i(t) := \frac{1}{\sqrt{\det S_i}}$, respectively, where S_i is a uniformly bounded positive definite weighted matrix and $\|x\|_S = \left(x^T S x\right)^{\frac{1}{2}}$. The matrices S_i are important to scale the energy of estimation error signals in order to make them comparable. In what follows, we refer to equation (42) as the dynamic weighting signal generator (DWSG).

We impose the constraint that the initial conditions $p_i(0)$ be chosen such that $p_i(0) \in (0,1)$ and $\sum_{i=1}^{N} p_i(0) = 1$. The parameters Q, R and the functions β_i, m_i are tuning parameters/functions of the CT-MMAE chosen by the designer based on the system being modeled.

IV. ILLUSTRATIVE EXAMPLE

A. Overview of the Simulator

In what follows we test our proposed observer using the Marine Cybernetics Simulator (MCSim), later on upgraded to Marine System Simulator (MSS). The MCSim is a modular multi-disciplinary simulator based on Matlab/Simulink. It was developed at the CeSOS. The MCSim incorporates high fidelity models, denoted as process plant model or simulation model in [24], at all levels (plants and actuators). It captures hydrodynamic effects, generalized coriolis and centripetal forces, nonlinear damping and current forces, and generalized restoring forces. It is composed of different modules such as environmental module, vessel dynamics module, thruster and shaft module, and vessel control module. For more details on the MCSim see [35], [36], [37], and [38].

In what follows, Monte-Carlo simulations are presented. A Continuous-Time Multiple-Model Adaptive Wave Filter (CT-MMAWF) is designed and simulated in section IV-B. In these simulations, the different environment conditions from calm to high seas are simulated using the spectrum of the Joint North Sea Wave Project (JONSWAP) [39]. Three different environment conditions from calm to high seas are considered, and for each one a separate observer is designed. Table I shows the definition of the sea condition associated with a particular model of supply vessel that is used in the MCSim.

TABLE I
DEFINITION OF SEA STATES FROM [40]

Sea States	DWF ω_0 (rad/s)	Significant Wave Height H_s (m)
Calm Seas	> 0.79	< 1.25
Moderate Seas	$[0.67\ 0.79]$	$[1.25\ 2.69]$
High Seas	$[0.45\ 0.67]$	$[2.69\ 9.71]$

B. Multiple Model Adaptive Wave Filter

In this simulation, it is assumed that the ship is subjected to wave disturbances with a fixed but unknown spectrum peak frequency in the interval $[0.45\ 0.85]\,rad/s$ covering sea states from calm and glassy to high seas. A set of three candidate values of the peak frequency are selected as $\{0.56, 0.73, 0.80\}\ rad/s$.[4]

[4]See [22] for a systematic way of choosing nominal parameters in MMAE.

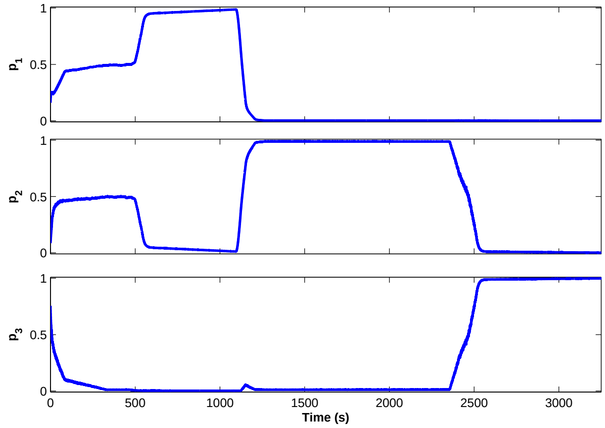

Fig. 3. Evolution of dynamic weights in multiple model adaptive wave filtering ($\omega_0 = 0.93\,rad/s$).

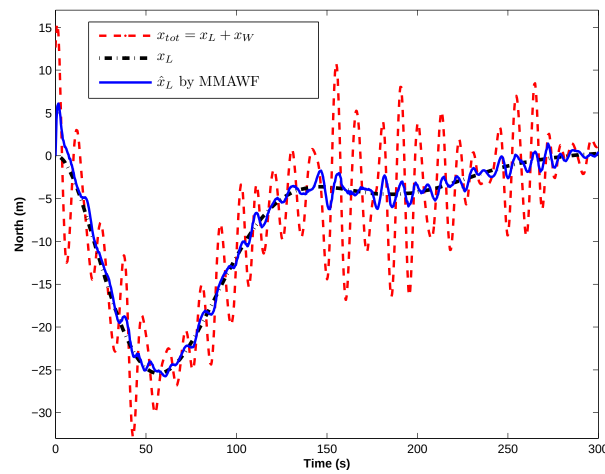

Fig. 4. Total motion, low frequency component of a (typical 100 meter long) DP vessel (only surge) and its estimate.

For each candidate value, a KF is developed based on the model described with (33)-(38) and a MMAE is derived with the dynamic weights given by (42). A nonlinear multivariable PID controller is designed that uses $\hat{\eta}_p$ and $\hat{\nu}$ provided by MMAE to control the position of the ship. Because the emphasis of this paper is not on control, but rather on filtering, we eschew the details of controller design.

Fig. 3 shows the dynamic weights in the multiple model adaptive wave filtering. In this simulation, in the first 500 seconds, the dominant wave frequency is $\omega_0 = 0.79$ (rad/sec). According to table I, this corresponds to the boundary of calm and moderate seas. During this interval of time, p_3 goes to zero while p_2 and p_3 stay close to 0.5; in the next 600 seconds the waves in the simulation are produced according to calm sea state ($\omega_0 = 0.84$). In the next 1100 seconds, the sea condition changes to moderate sea and in the last 1100 second, the waves are produced to simulate high sea condition. Fig. 3 shows that the dynamic weights adaptively track the changes in the sea state. Figs. 4 shows the time evolution of the total motion, the low frequency component of the motion, and low frequency motion estimates by the CT-MMAWF in high sea state.

V. CONCLUSIONS AND FUTURE WORK

This paper proposed a new technique for adaptive wave filtering, with application to DP. Its key contribution was the development of a modified model for wave filtering and the use of MMAE techniques to yield a filter that adapts to sea state variations. Future work will include the application of the method developed to model test experiments.

VI. ACKNOWLEDGMENTS

We thank our colleagues Øyvind Smogeli, N. T. Dong and Thor I. Fossen for many discussions on wave filtering and adaptive estimation.

REFERENCES

[1] J. Balchen, N. A. Jenssen, and S. Sælid, "Dynamic positioning using Kalman filtering and optimal control theory," in *the IFAC/IFIP Symposium On Automation in Offshore Oil Field Operation*, Bergen, Norway, 1976, pp. 183–186.

[2] ——, "Dynamic positioning of floating vessels based on Kalman filtering and optimal control," in *Proc. of the 19th IEEE Conference on Decision and Control*, New York, NY, 1980, pp. 852–864.

[3] ——, "A dynamic positioning system based on Kalman filtering and optimal control," *Modeling, Identification and Control (MIC)*, vol. 1, no. 3, pp. 135–163, 1980.

[4] M. J. Grimble, R. J. Patton, and D. A. Wise, "The design of dynamic ship positioning control systems using stochastic optimal control theory," *Optimal Control Applications and Methods*, vol. 1, pp. 167–202, 1980.

[5] ——, "The design of dynamic ship positioning control systems using stochastic optimal control theory," *IEE Proceedings*, vol. 127, no. 3, pp. 93–102, 1980.

[6] S. Sælid, N. A. Jenssen, and J. Balchen, "Design and analysis of a dynamic positioning system based on Kalman filtering and optimal control," *IEEE Transactions on Automatic Control*, vol. 28, no. 3, pp. 331–339, 1983.

[7] T. I. Fossen, S. I. Sagatun, and A. J. S. rensen, "Identification of dynamically positioned ships," *Journal of Control Engineering Practice*, vol. 4, no. 3, pp. 369–376, 1996.

[8] A. J. Sørensen, S. I. Sagatun, and T. I. Fossen, "Design of a dynamic positioning system using model-based control," *Journal of Control Engineering Practice*, vol. 4, no. 3, pp. 359–368, 1996.

[9] Å. Grøvlen and T. I. Fossen, "Nonlinear control of dynamic positioned ships using only position feedback: An observer backstepping approach," in *Proc. IEEE Conference on Decision and Control (CDC'96)*, Kobe, Japan, 1996.

[10] J. P. Strand, "Nonlinear position control systems design for marine vessels," Ph.D. dissertation, Dept. of Eng. Cybernetics, Norwegian University of Science and Technology, Trondheim, Norway, 1999.

[11] T. I. Fossen, "Nonlinear passive control and observer design for ships," *Modeling, Identification and Control (MIC)*, vol. 21, no. 3, pp. 129–184, 2000.

[12] G. Torsetnes, J. Jouffroy, and T. I. Fossen, "Nonlinear dynamic positioning of ships with gain-scheduled wave filtering," in *Proc. IEEE Conference on Decision and Control (CDC'04)*, Paradise Island, Bahamas, 2004.

[13] A. J. Sørensen, "A survey of dynamic positioning control systems," *Annual Reviews in Control*, vol. 35, pp. 123–136, 2011.

[14] T. I. Fossen, *Handbook of Marine Craft Hydrodynamics and Motion Control*. Chichester, UK: John Wiley & Sons. Ltd, 2011.

[15] T. D. Nguyen, A. J. Sørensen, and S. T. Quek, "Design of hybrid controller for dynamic positioning from calm to extreme sea conditions," *Automatica*, vol. 43, no. 5, pp. 768–785, 2007.

[16] T. I. Fossen and J. P. Strand, "Passive nonlinear observer design for ships using lyapunov methods: Full-scale experiments with a supply vessel," *Automatica*, vol. 35, pp. 3–16, 1999.

[17] J. P. Strand and T. I. Fossen, "Nonlinear passive observer for ships with adaptive wave filtering," *New Directions in Nonlinear Observer Design (H. Nijmeijer and T. I. Fossen, Eds.), Springer-Verlag London Ltd.*, pp. 113–134, 1999.

[18] V. Hassani, A. M. Pascoal, A. P. Aguiar, and M. Athans, "A multiple model adaptive wave filter for dynamic ship positioning," in *Proc. the IFAC Conf. on Control Appl. in Marine Systems (CAMS10)*, Rostock, Germany, September 2010.

[19] B. D. O. Anderson and J. B. Moore, *Optimal Filtering*. New Jersey, USA: Prentice-Hall, 1979.

[20] A. P. Aguiar, V. Hassani, A. M. Pascoal, and M. Athans, "Identifcation and convergence analysis of a class of continuous-time multiple-model adaptive estimators," in *Proc. of The 17th IFAC World Congress*, Seoul, Korea, Jul. 2008.

[21] V. Hassani, A. P. Aguiar, M. Athans, and A. M. Pascoal, "Multiple model adaptive estimation and model identification using a minimum energy criterion," in *Proc. ACC'09 - American Control Conference*, St. Louis, Missouri, USA, 2009.

[22] V. Hassani, A. P. Aguiar, A. M. Pascoal, and M. Athans, "A performance based model-set design strategy for multiple model adaptive estimation," in *ECC'09 - European Control Conference*, Budapest, Hungary, 2009.

[23] ——, "Further results on plant parameter identification using continuous-time multiple model adaptive estimators," in *Proc. IEEE Conference on Decision and Control (CDC'09)*, Shanghai, China, 2009.

[24] A. J. Sørensen, "Lecture notes on marine control systems," Norwegian University of Science and Technology, Tech. Rep. Report UK-11-76, 2011.

[25] M. S. Triantafyllou, "Cable mechanics for moored floating systems," in *Proc. of 7th International Conference on the Behaviour of Offshore Structures at Sea (BOSS'94)*, Cambridge, MA, 1994, pp. 57–77.

[26] O. M. Faltinsen, *Sea Loads on Ships and Offshore Structures*. Cambridge, UK: Cambridge University Press, 1990.

[27] A. Loria, T. I. Fossen, and E. Panteley, "A separation principle for dynamic positioning of ships: theoretical and experimental results," *IEEE Trans. on Contr. Syst. and Tech.*, vol. 8, no. 2, pp. 332–343, 2000.

[28] T. I. Fossen and T. Perez, "Kalman filtering for positioning and heading control of ships and offshore rigs," *IEEE Control Systems Magazine*, vol. 29, no. 6, pp. 32–46, December 2009.

[29] D. T. Magill, "Optimal adaptive estimation of sampled stochastic processes," *IEEE Trans. on Automat. Contr.*, vol. 10, pp. 434–439, 1965.

[30] Y. Baram and N. Sandell, "An information theoretic approach to dynamical systems modeling and identification," *IEEE Trans. on Automat. Contr.*, vol. 23, pp. 61–66, 1978.

[31] D. G. Lainiotis, "Optimal adaptive estimation: Structure and parameter adaptation," *IEEE Trans. on Automat. Contr.*, vol. 16, pp. 160–170, 1971.

[32] K.-P. Dunn and I. B. Rhodes, "A generalized representation theorem with applications to estimation and hypothesis testing," in *11th Annual Allerton Conf. on Circuit and System Theory*, 1973.

[33] K.-P. Dunn, "Measure transformation, estimation, detection and stochastic control," Ph.D. dissertation, Washington University, St. Louis, MO, USA, 1974.

[34] A. P. Aguiar, M. Athans, and A. Pascoal, "Convergence properties of a continuous-time multiple-model adaptive estimator," in *Proc. of ECC'07 - European Control Conference*, Kos, Greece, Jul. 2007.

[35] A. J. Sørensen, E. Pedersen, and O. Smogeli, "Simulation-based design and testing of dynamically positioned marine vessels," in *Proc. of International Conference on Marine Simulation and Ship Maneuverability (MARSIM'03)*, Kanazawa, Japan, 2003.

[36] T. Perez, O. N. Smogeli, T. I. Fossen, and A. J. Sørensen, "An overview of marine systems simulator (MSS): A simulink toolbox for marine control systems," in *Proc. of Scandinavian Conference on Simulation and Modeling (SIMS'05)*, Trondheim, Norway, 2005.

[37] T. Perez, A. J. Sørensen, and M. Blanke, "Marine vessel models in changing operational conditions a tutorial," in *14th IFAC Symposium on System Identification (SYSID'06)*, Newcastle, Australia, 2006.

[38] T. I. Fossen and T. Perez, "Marine systems simulator (MSS)," "www.marinecontrol.org", 2009.

[39] K. Hasselmann, T. P. Barnett, E. Bouws, H. Carlson, D. Cartwright, K. Enke, J. A. Ewing, H. Gienapp, D. E. Hasselmann, P. Kruseman, A. Meerburg, P. Müller, D. J. Olbers, K. Richter, W. Sell, and H. Walden, "Measurements of wind-wave growth and swell decay during the joint north sea wave project (JONSWAP)," *Ergnzungsheft zur Deutschen Hydrographischen Zeitschrift Reihe*, vol. 8, no. 12, pp. 1–95, 1973.

[40] W. G. Price and R. E. D. Bishop, *Probabilistic Theory of Ship Dynamics*. London, UK: Chapman and Hall, 1974.